3.1 SPATIAL CHARACTERISTICS OF POWER VARIABILITY FROM A LARGE WIND FARM IN IOWA DURING THE 2013 CROP/WIND ENERGY EXPERIMENT (CWEX-13)

Daniel. A. Rajewski[1*], Eugene S. Takle[1], Julie K. Lundquist[2, 3], Samantha L. Irvin[1], and Russell K. Doorenbos[1]

[1]Iowa State University, Ames, Iowa
[2]University of Colorado, Boulder, Colorado
[3]National Renewable Energy Laboratory, Golden, Colorado

1. INTRODUCTION

Wind farm wakes remain a challenging aspect of both aerodynamic simulation and the design of future wind farms and forecast assessment of current onshore wind farms in the U.S. (e.g. U.S. DOE, 2008). At night, strong stable stratification hinders the recovery of the wind profile in the wake because of the absence of turbulence above and within the turbine rotor layer (Wharton and Lundquist 2012). Nearby turbines from parent wakes may experience power reductions of 20-40% in these low-turbulence and shear conditions of upwind wakes (Wharton and Lundquist 2011, Vanderwende and Lundquist 2012; Takle et al. 2014). In addition to their thermal stability, wakes are complicated by the horizontal in-row and between-row spacing of turbines (e.g. Meyers and Meneveau 2012, Archer et al. 2013, Gaumond et al. 2014). Ambient inflow speed and turbulence also impact loading stresses on turbine components and the production of turbine-generated turbulence (Churchfield et al. 2012, Hansen et al. 2012, Clifton et al. 2013). These meteorological factors of the ambient flow (stability, direction, speed, turbulence) influence wake properties of dissipation and/or combination with nearby wakes (Frandsen et al. 2007, Keck et al. 2014).

Calibration data for numerical simulations of utility-scale wind farms are scarce and turbine Supervisory Control and Data Acquisition (SCADA) data are not easily obtained from wind energy companies. Remote sensing data from LiDAR, SoDAR or Doppler radar have shown increasing application in detecting wake losses over limited spatial scales (Rhodes and Lundquist 2013, Hirth and Schroeder 2013, Aitken et al. 2014, Lundquist et al. 2014,). The Crop Wind Energy Experiment of 2013 (CWEX-13) provides a framework to compare field observations of LiDAR, surface flux stations, and wind farm SCADA to determine spatial distributions of wake losses within a large wind farm in Iowa. Our results will quantify these losses according to the approaching wind direction, the geometric orientation of the wind farm, the distance between turbines, elevation, and the variability of surface layer stratification.

* *Corresponding author address*: Daniel A. Rajewski, Iowa State Univ., Dept. of Agronomy, Ames, IA 50011; email: drajewsk@iastate.edu

2. MATERIALS AND METHODS

Surface fluxes and LiDAR measurements were taken in CWEX-13 during late June through mid-September in several soybean fields throughout the northwest third of turbines in a 300 MW Iowa wind farm as in Fig. 1. The turbines, with 80-m hub height (H) and 82-m rotor diameters (D), are arrayed from northwest to southeast, which are also the prevailing winds in the winter and summer months. Measurement configuration and instrumentation for the flux stations and LiDARs are similar as described in Rajewski et al. (2013 and 2014a) but with higher mounted sonic anemometers (8m above the ground level). Turbine SCADA wind speed, yaw angle, power, temperature, and blade pitch from 83 of the 200 total turbines were provided by the owner of the wind farm for the same period as the field measurements.

We categorize differences in the normalized power from a reference turbine in the leading turbine line in the southern portion of the CWEX-13 study area. We denote this turbine power as P_0, and the normalized differences with comparison to the other 82 turbines (P_i) calculated as in eq. (1):

$$\Delta P_i = \frac{P_i - P_0}{P_0} * 100\% \quad (1)$$

Normalized power differences are calculated for each of the remaining 82 turbines for every 10-min period. We filter out observations when the leading line of turbines has any turbine less than 50 kW of power generation upwind (Rajewski et al. 2014a). We recognize other turbine operation characteristics (hub height wind speed, blade pitch) will influence wakes; however, our intention is to offer a preliminary scope of wake wind direction and stability impacts over a large array of wind turbines. We also filter the power differences when the upwind reference LiDAR 80-m wind speed is less than 3.5 ms^{-1} (Rhodes and Lundquist 2013) or when the surface flux stations record any precipitation or error warnings from the flux station sonic anemometers. The remainder of the quality-controlled observations, about 80% of the total period of the experiments, is sorted by the reference station surface stratification and the undisturbed hub height wind direction.

We determine the Obukhov length at the reference flux station (ISU 2) upwind of the leading line of turbines and relate the stability according to the stability classes (cL) determined by Hansen et al. (2012). Strongly stable (cL=4) and strongly unstable conditions (cL=-4) are also included in our group categories of stability (Stable, Neutral, and Unstable as adopted by Mirocha et al. 2015 (in review) and described in Table 1). Rajewski et al. (2014b) determined that the strength of the stability is less important than the stability sign and so the weaker stable and unstable categories are grouped into the neutral category. For the hub-height ambient wind direction we designate wind directional categories according to the reference LiDAR (CU-1) wind direction at 80m. The categories are apportioned for different sizes of wake wind direction angles according to the method of Barthelmie et al. 2010 for individual turbines and from other CWEX campaigns (e.g. Rajewski et al. 2013, Rajewski et al. 2014a). We depict in Table 2 wake direction categories, ranges of wind direction, wake interpreting characteristics, and the number of observations for each of the three stability categories. Among most wind directions, except for westerly and easterly winds, we have 100-750 events to determine areal mean composites of normalized power differences. A series of maps with these mean composites demonstrate the different wake characteristics throughout the wind farm for multiple stability and wind direction categories.

3. RESULTS

We first determine any directional variability in wake losses for conditions with weak to no thermal stratification. In agreement with several numerical and wind tunnel simulations, the pattern of normalized power differences is less than ±10% of the reference turbine for most turbines separated by a distance of >10 D. Power is reduced by 20-30% only for turbines located within 5-7 D of nearby turbines as shown in Fig. 2a for southeasterly winds, and this waking pattern shows similar agreement with simulations. For more southerly winds there are several turbines on the west edge of the farm that are producing upward of 20% higher power than those in the middle of the complex (Fig. 2b). This demonstrates the areal extent of wakes from the south phase of the wind farm moving into the eastern edge of the turbines but not the western side.

For southwesterly winds in Fig. 2c we notice less power variability except for the pocket of turbines that are in the southwestern portion of the study area. Power losses of 10-15% are associated with lower elevation upwind of the farm. As indicated in Fig. 1, a 40-m difference in terrain exists between the southwest border of the farm and the center portion closest to the ISU 7 and ISU 5 flux stations.

In northwest winds the northern most two to three lines of turbines are producing 20-30% more power than those at the southern edge of the wind farm (Fig. 2d). The enhancement of power at the north end of the wind farm indicates the importance of the upwind fetch and the 30-40-m higher elevation difference than for winds moving through the central and southern portions of the wind farm. However, in the central portion of the wind farm wake losses approach 30% for turbines located within 10D of nearby turbines. There is no consistent feeding of wakes from northerly turbines into southerly turbines to demonstrate a larger power reduction at the south end of the farm. Therefore, the bulk of the power differences are solely from the influence of terrain in conditions of neutral stratification.

For unstable stratification (figure not shown), wake losses follow similar magnitude and position as for near-neutral stability. The turbines with 20-30% lower power than the reference turbine are within 10D of other turbines with a leading turbine waking two consecutive turbines for southeasterly flow. For other areas of the wind farm, wake losses are within ±10-15% as we would expect the unstable stratification to decrease the downwind distance of wake dissipation. Slightly higher power ratios (within 5%) occur on the northeastern border of the wind farm, whereas there is some hint of aggregate wake loss in turbines located in the southeastern edge of the CWEX-13 array from multiple wakes south of the study area. Similar patterns are observed as for neutral non-terrain-induced pockets of higher wake loss when turbine spacing is <10D. Wake meandering is a possible influence on power in unstable stratification; however, we cannot determine losses due to meandering and yaw with 10-minute temporal resolution.

In stable conditions there is both the factors of wakes and elevation in controlling the power losses. The influence of each factor depends heavily on the wind direction approaching the wind farm and the orientation of turbines with respect to nearby turbines in this farm. For southeasterly winds (Fig. 3a), the northwest and extreme southern lines of turbines indicate similar power enhancements from the reference turbine line. With these regions producing 40-60% higher power, we are able to outline the perceived influence of multiple wakes from several lines of turbines. Wake losses in this aggregate wake-sheet are between 20-30% except for the small pocket of turbines in the center portion of the farm in which the most downwind turbine has a 40-50% reduction from P_0. The wakes over the central portion of the farm appear to reach a wake-dissipation distance between the second and third most northern lines of turbines. The highest power ratio in the first and second line likely describes non-turbine influence on upward fetch and the importance of 30-40m higher elevation, and therefore higher hub height speeds.

For winds from the south-southeast in Fig. 3b, there is continuing evidence of this aggregate wake channel as higher power ratios are evident for turbines in the southwestern edge of the wind farm. Wakes from the extreme southern phase of the wind farm are moving through entire wind farm to the northern most two lines of turbines. Power losses are 30-40% a few lines north of the reference turbine, whereas some reduction of the wake strength occurs with downwind distance to the northern two lines of turbines. We see less importance on the role of elevation in changing the wind resource for turbines at the northern edge of the farm compared to southeast flow. Wakes are therefore persistent in orientation and intensity while moving through the bulk of the turbines in the farm for stable stratification.

For southwest winds, the subtle differences in elevation between the north and south end of the farm illustrate the isolated power enhancements on the westernmost turbines in the northern two lines (Fig. 3c). Power is reduced by 20-30% for the southwest portion of the farm and again we refer to the 20-30m lower terrain to explain this feature. The majority of turbines on the eastern and central portions of the wind farm have wake losses within ±10-15%. The southeast portion of the wind farm has higher terrain than the patch of land upstream of the southwestern set of turbines. However, wake-induced losses are not as large as for turbines on the southwestern border. Therefore the importance of fetch and elevation dominate the power losses in this portion of the wind farm.

In the last case of northwesterly flow in Fig. 3d, we again observe the higher power ratios in the northern most turbine lines as compared to the southern region of turbines. We believe a combination of wake and terrain effects are important in determining the wake losses. As in the neutral case, the largest reductions of 40-50% occur in the small pocket of turbines located diagonally in the center portion of the farm. Outside of this region of turbines, wakes are slowing the wind for turbines in the southeast part of the study area. Unlike a gradual tapering off of the power loss as observed in offshore wind farms (e.g. Barthlemie et al. 2009, 2010; Barthelmie and Jensen 2010), we observe a 20% lower power at the southeast region of the farm than at the reference turbine. We believe these losses are also linked to terrain because the elevation difference within the two locations is about 20-30 m.

4. CONCLUSIONS

We analyze wake losses in a large wind farm by considering stratification and wind direction in calculating normalized power ratios with respect to a reference turbine in the southern portion of CWEX-13 array. In agreement with several numerical and wind tunnel simulations, wake losses are generally within ±10-15% for different approaching wind directions to the wind farm in neutral conditions. Our results, however, suggest a mix of above and below reference turbine power generation in nighttime stable conditions. Wake losses are complicated with respect to orientation of the wind farm and terrain changes. We do observe an aggregation of wakes at the northwest portion of the farm for southeasterly winds; however, the northernmost turbines, which are not influenced by wakes and in 30-40m higher terrain, yield at least 50% more power than the reference turbine on the lower elevation. Our results demonstrate that even under relatively smooth terrain of the agricultural surfaces of the U.S. Midwest, power losses result from both turbine wakes and from elevation variability. Future analyses will determine additional factors of hub height wind speed and blade pitch on these wake losses.

Acknowledgements: CWEX-13 was supported in part by the National Renewable Energy Laboratory under Professor Lundquist's Joint Appointment. Support for ISU flux station instrumentation deployment was provided by National Science Foundation under the State of Iowa EPSCoR Grant 1101284 and undergraduate student participation was supplemented by funding from an NSF Research Experience for Undergraduates program under grant 1063048. Data analysis was supported in part by the National Science Foundation under the State of Iowa EPSCoR Grant 1101284. The authors also acknowledge the wind farm owner for the use of the SCADA data.

5. REFERENCES

Aitken, M. L., B. Kosović, J. D. Mirocha, and J. K. Lundquist, 2014: Large eddy simulation of wind turbine wake dynamics in the stable boundary layer using the Weather Research and Forecasting Model. *J. Renew. Sustain. Energ.*, **6**, 033137.

Archer, C. L., S. Mirzaeisefat, and S. Lee, 2013: Quantifying the sensitivity of wind farm performance to array layout options using large-eddy simulation. *Geophys. Res. Lett.*, **40**, 4963-4970.

Barthelmie, R. J., K. Hansen, S. T. Frandsen, O. Rathmann, J. G. Schepers, W. Schlez, J. Phillips, K. Rados, A. Zervos, E. S. Politis, and P. K. Chaviaropoulos, 2009: Modelling and measuring flow and wind turbine wakes in large wind farms offshore. *Wind Energ.*, **12**, 431–444. doi: 10.1002/we.348

Barthelmie, R. J., and L. E. Jensen, 2010: Evaluation of wind farm efficiency and wind turbine wakes at the Nysted offshore wind farm. *Wind Energ*, **13**, 573-586.

Barthelmie, R. J., S. C. Pryor, S. T. Frandsen, K. S. Hansen, J. G. Schepers, K. Rados, W. Schlez, A. Neubert, A., L. E. Jensen, and S. Neckelmann,

2010: Quantifying the impact of wind turbine wakes on power output at offshore wind farms. *J. Atmos. Oceanic Technol*., **27**, 1302-1317. doi: 10.1175/2010JTECHA1398.1.

Churchfield, M. J., S. Lee, J. Michalakes, and P. J. Moriarty. 2012. A numerical study of the effects of atmospheric and wake turbulence on wind turbine dynamics. *J. Turbulence* **13**, 1-32.

Clifton, A., S. Schreck, G. Scott, N. Kelley and J.K. Lundquist, 2013: Turbine Inflow Characterization at the National Wind Technology Center. J*. Solar Energ. Engineer*., **135**, 031017.

Frandsen, S. T., R. J. Barthelmie, O. Rathmann, H. E. Jørgensen, J. Badger, K. S. Hansen, S. Ott, P.-E. Rethore, S. E. Larsen, and L. E. Jensen, 2007: Summary report: The shadow effect of large wind farms: measurements, data analysis and modelling. Risø National Laboratory report number 1615(EN).

Gaumond, M., P.E. Réthoré, S. Ott, A. Peña, A. Bechmann, A., K.S. Hansen, 2014: Evaluation of the wind direction uncertainty and its impact on wake modeling at the Horns Rev offshore wind farm. *Wind Energ*, **17**, 1169-1178.

Hansen, K.S., R. J. Barthelmie, L.E. Jensen and A. Sommer, 2012: The impact of turbulence intensity and atmospheric stability on power deficits due to wind turbine wakes at Horns Rev wind farm. *Wind Energ.* **15**, 183196.

Hirth, B.D., and J.L. Schroeder, 2013: Documenting wind speed and power deficits behind a utility-scale wind turbine. *J. Appl. Meteor. Climatol.* **52**, 39–46. doi: 10.1175/JAMC-D-12-0145.1.

Keck, R. E., M. Maré, M. J. Churchfield, S. Lee, G. Larsen, and M. H. Aagaard, 2014: On atmospheric stability in the dynamic wake meandering model. *Wind Energ*., **17**, 1689-1710.

Lundquist, J. K., E. S. Takle, M. Boquet, B. Kosović, M. E. Rhodes, D. Rajewski, R. K. Doorenbos, S. Irvin, M. K. Aitken, K. Friedrich, P.T. Quelet, J. Rana, C. St. Martin, B. Vanderwende, and R. Worsnop, 2014: Lidar observations of interacting wind turbine wakes in an onshore wind farm. EWEA meeting proceedings.

Meyers, J., and C. Meneveau, 2012: Optimal turbine spacing in fully developed wind-farm boundary layers, *Wind Energ.*, **15**, 305-317. doi:10.1002/we.469.

Mirocha, J. D., D. A. Rajewski, N. Marjanovic, J. K. Lundquist, B. Kosović, C. Draxl, and M. J. Churchfield, 2015: Investigating wind turbine impacts on near-wake flow using profiling lidar and data and large-eddy simulations with an actuator disk model (In review at *Journal of Renewable and Sustainable Energy*).

Rajewski D. A., E. S. Takle, J. K. Lundquist, J. H. Prueger, R. Pfeiffer, J. L. Hatfield, K. K. Spoth, and R. K. Doorenbos, 2014: Changes in fluxes of heat, H2O, and CO2 caused by a large wind farm. *Agric For Meteor.* **194**, 175–187. doi: 10.1016/j.agrformet.2014.03.023

Rajewski, D. A., E. S. Takle, J. K. Lundquist, M. E. Rhodes, S. L. Irvin, and R. K. Doorenbos: 2014. Impacts of stable stratification on turbine flow and wake characteristics: Lessons from the Crop/Wind-Energy Experiments (CWEX). International Energy Agency Research and Development Task XI Topical Expert Meeting #78, Lubbock, 8 Oct., 2014.

Rhodes, M. E., and J. K. Lundquist, 2013: The effect of wind turbine wakes on summertime Midwest atmospheric wind profiles. *Bound.-Layer Meteor.* **149**, 85-103. doi:10.1007/s10546-013-9834-x.

Takle, E. S., D. A. Rajewski, J. K. Lundquist, W. A. Gallus Jr, and A. Sharma, 2014: Measurements in support of wind farm simulations and power forecasts: The Crop/Wind-energy Experiments (CWEX). In *J. Phys. Conf. Series*, **524**, 012174. IOP Publishing. doi: 10.1088/1742-6596/524/1/012174

Vanderwende, B. and J. K. Lundquist. 2012: The modification of wind turbine performance by statistically distinct atmospheric regimes. *Environ. Res. Lett.* **7**, 034035 doi:10.1088/1748-9326/7/3/034035.

Wharton, S. and J. K. Lundquist, 2012: Assessing atmospheric stability and its impacts on rotor-disk wind characteristics at an onshore wind farm. *Wind Energ*., **15**, 525–546. doi: 10.1002/we.483.

U.S. DOE Office of Energy Efficiency and Renewable Energy, 2008: 20% Wind Energy by 2030: Increasing Wind Energy's Contribution to U.S. Electricity Supply, 248 pp.; NREL Report No. TP-500-41869; DOE/GO-102008-2567. *[Available online at* http://www.nrel.gov/docs/fy08osti/41869.pdf.]

6. ILLUSTRATIONS AND TABLES

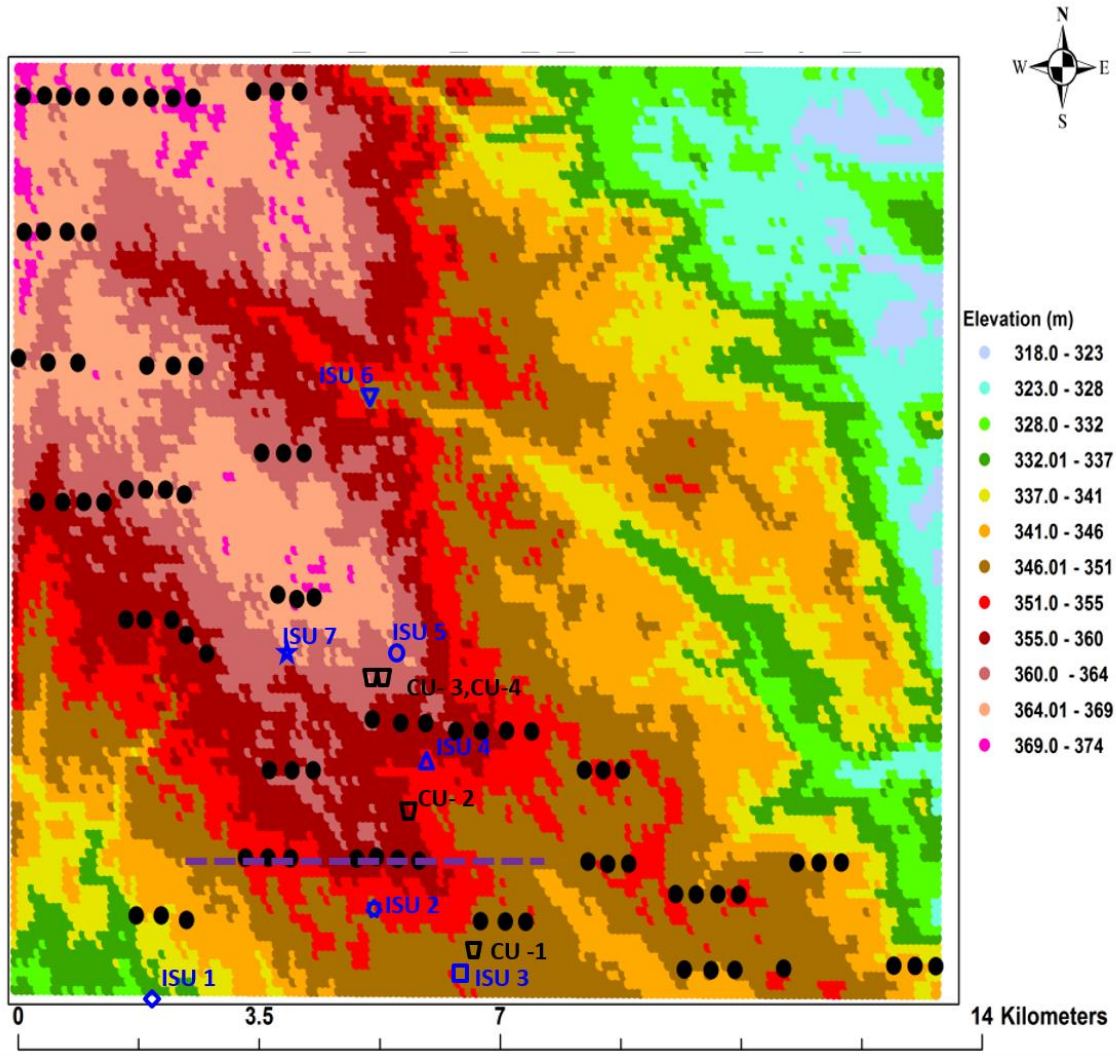

Fig. 1. Turbine locations, flux stations and LiDARs placement for CWEX-13. Distances of flux stations and LiDARs from the reference turbine line are denoted in red.

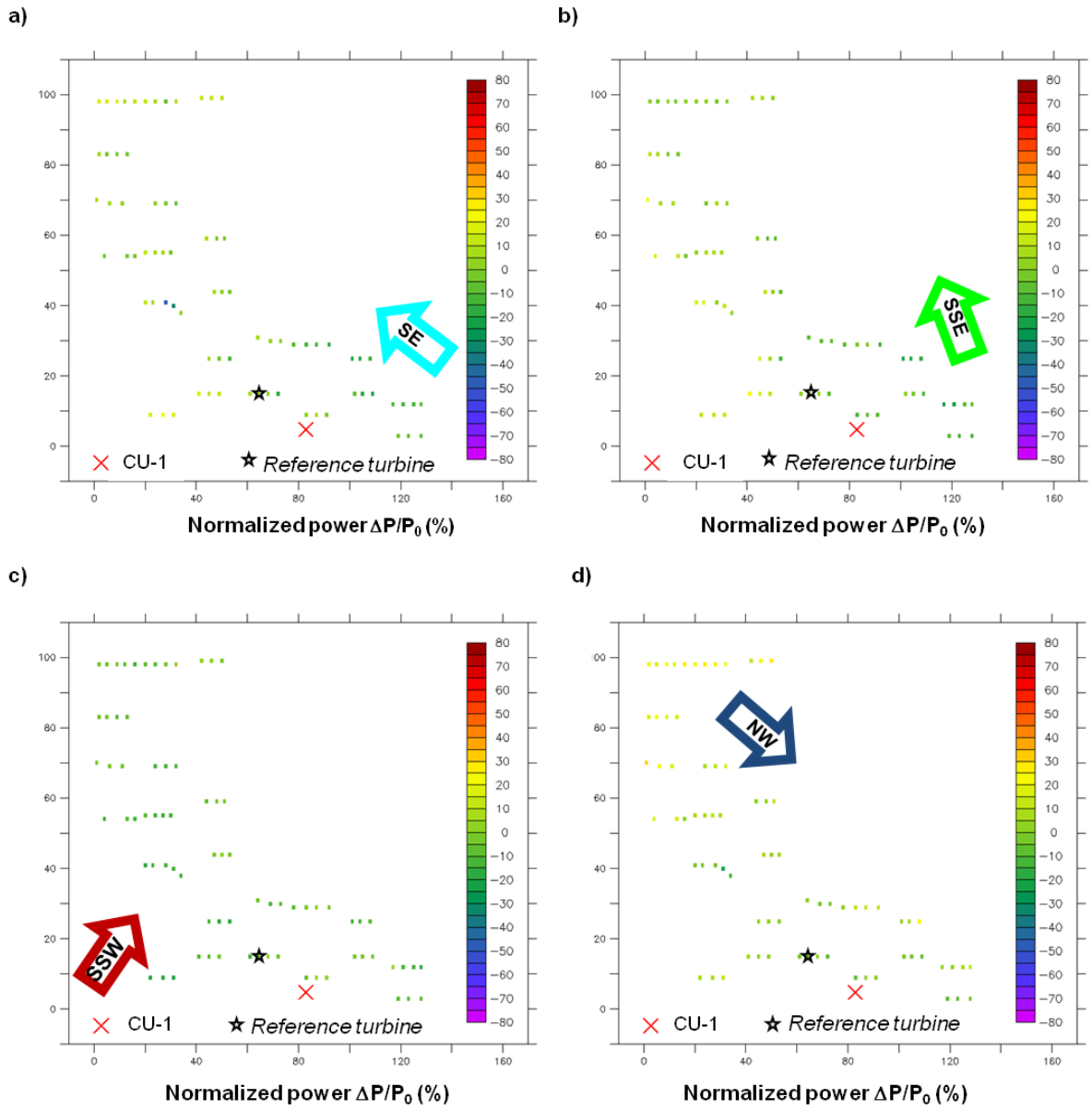

Fig. 2. Normalized power differences for the wind farm sorted by the ISU 2 reference flux station neutral stratification for the upwind CU-1 LiDAR, 80-m wind directions in a) southeast winds, b) south-southeast winds, c) south-southwest winds, and d) northwest winds.

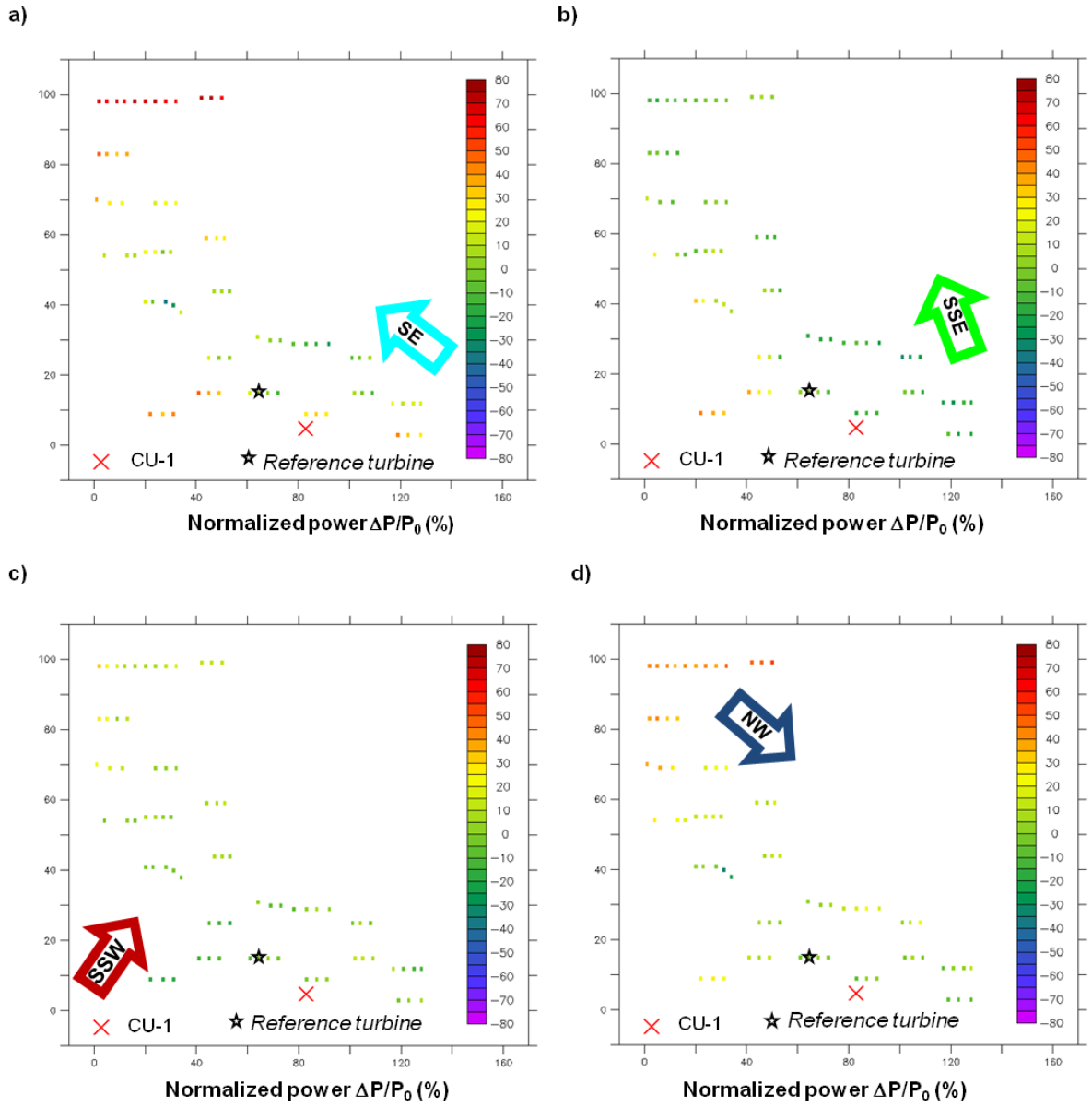

Fig. 3. Normalized power differences for the wind farm sorted by the reference ISU 2 flux station stable stratification for the upwind CU-1 LiDAR, 80-m wind directions in a) southeast winds, b) south-southeast winds, c) south-southwest winds, and d) northwest winds.

Stability Class	Obukhov length (m)	Stability category (Hansen et al. 2012)	Stability category (Mirocha et al. 2015)
cL=-4	-50<L<0	---	Unstable
cL=-3	-100 ≤ L ≤ -50	Very unstable	Unstable
cL=-2	-200 ≤ L ≤ -100	Unstable	Unstable
cL=-1	-500 ≤ L ≤ -200	Near unstable	Neutral
cL=0	|L|>500	Neutral	Neutral
cL=1	200 ≤ L ≤ 500	Near stable	Neutral
cL=2	50 ≤ L ≤ 200	Stable	Stable
cL=3	10 ≤ L ≤ 50	Very stable	Stable
cL=4	0<L<50	---	Stable

Table 1. ISU 2 reference flux station stability classes and corresponding Obukhov length and stability categories determined by Hansen et al. 2012. Stability categories used in this analysis are grouped according to the method adopted in Mirocha et al. 2015.

CU-1 80-m wind direction category	Direction bin (°)	Turbine wake category	# of observations (Stable)	# of observations (Neutral)	# of observations (Unstable)
N-NNE	345-0, 0-15	multiple lines	467	163	276
NE	45-85	few lines	111	10	30
E-ESE	85-115	long lines	7	1	2
SE	115-145	many lines	105	62	127
SSE	145-165	few lines	246	103	185
S	165-195	few lines	728	176	409
SSW	195-215	few lines	413	95	303
SW	215-235	few lines	334	151	159
WSW	235-265	few turbines	142	76	97
W-WNW	265-295	long lines	77	8	19
NW	295-345	many lines	103	45	249

Table 2. Reference LiDAR CU-1 80-m wind direction category, wind direction window, turbine wake category, and number of observations for each directional category with stable, neutral, and unstable conditions as determined from the surface stability at the ISU 2 reference flux station.